Space Environment and Effects Tool (SEET) for Ansys STK 12.9.1: Scientific Background

This document discusses the scientific background of the Space Environment and Effects Tool (SEET) and its various modules. It also provides an overview of user-selectable options within each module in the System Tool Kit (STK) application.

Contents

Introduction

AER's Space Environment and Effects Tool (SEET) is an add-on software module for Ansys's System Tool Kit (STK). It provides comprehensive modeling of the space environment and prediction capabilities of ambient near-Earth environment effects on space vehicles. Extensive information on space environments and the vehicles travelling through them is offered in their respective modules:

- Trapped Radiation Environment
  - Radiation Environment
  - South Atlantic Anomaly (SAA) Transit
- Untrapped Radiation Environment
  - Galactic Cosmic Ray (GCR)
  - Solar Energetic Particle (SEP)
- Particle Flux
  - Meteor Environment
  - Debris Environment
- Vehicle Temperature
- Magnetic Field

Some models supporting the Radiation Environment, SAA Transit, and Magnetic Field capabilities are adapted from the Air Force Research Laboratory (AFRL) AF-GEOSpace Version 2.1P software suite. The Radiation Environment capabilities have been augmented with the recent addition of the new IRENE AE9/AP9 model.

The Particle Flux module is adapted from the Meteor Impact module in AF-GEOSpace and extended to include orbital debris.

Most SEET capabilities provide climatological information on the state of the space environment based on the binning and averaging of large amounts of historical data. Climatological information is most useful for satellite designers and mission planners that need to anticipate environmental factors over a multi-year mission, or to perform trade studies for different orbits and instrumentation shielding strategies for best and worst-case radiation exposures.

Radiation Environment

Earth's radiation environment is primarily composed of naturally occurring charged particles trapped in the Earth's magnetic field in regions known as the Van Allen belts. The Van Allen radiation belt particles are responsible for most of the long-term ionizing-dose damage to satellite electronics and materials.

Solar energetic particles (SEPs) and galactic cosmic rays (GCRs) also contribute to the natural radiation environment. GCRs and SEPs during solar storms are significant of single event effects (SEEs) and single event upsets (SEUs) which result in instantaneous upsets and glitches in the operation of satellite electronics.

Information on satellite dosage and incident energetic particle flux is critical to satellite designers and mission planners as satellite devices degrade over time due to the collected dose. The total dose is computed by integrating the instantaneous dosage rate over time. The dosage rate itself depends on the incident energetic particle flux and shielding parameters of a shielded instrument such as material type and thickness.

The SEET Radiation Environment module computes the expected dosage rate and accumulated dose (i.e., ionizing energy deposition) due to energetic electron and proton particle fluxes. These are computed for a range of user-specified shielding thicknesses. It also computes the energetic proton and electron fluxes for a wide range of particle energies.

Trapped Radiation Environment

The Trapped Radiation Environment module offers a set of radiation models and two further components: Radiation Models and Southern Atlantic Anomaly (SAA).

Figures 1 and 2 below illustrate the electron and proton flux in the trapped radiation (Van Allen) belt.

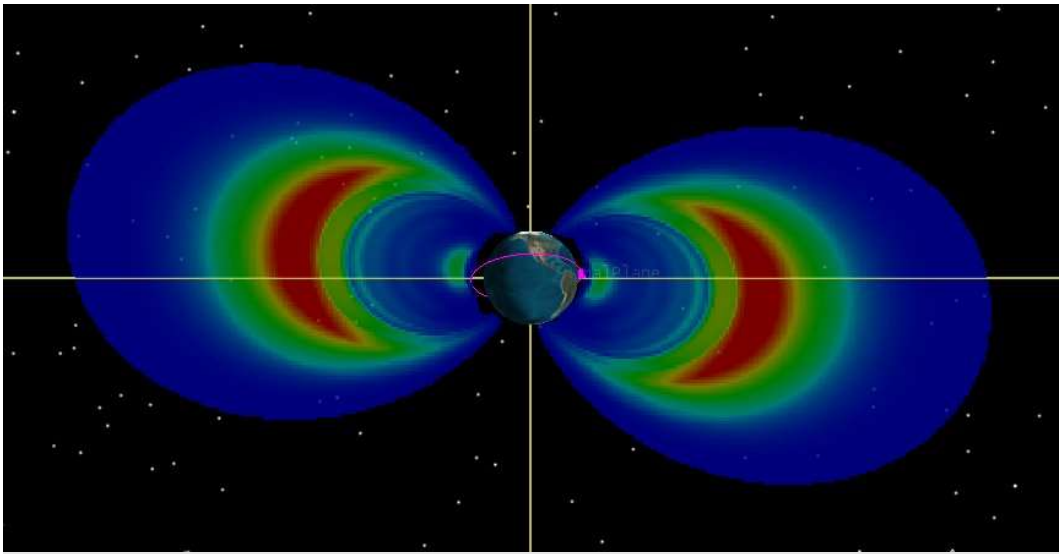

Figure 1. *Electron radiation flux cross-section for particles at 0.95 MeV based on the NASA AE8 model. Higher values are concentrated in two belts, the Van Allen radiation belts. (Figure courtesy of AER, Inc.)*

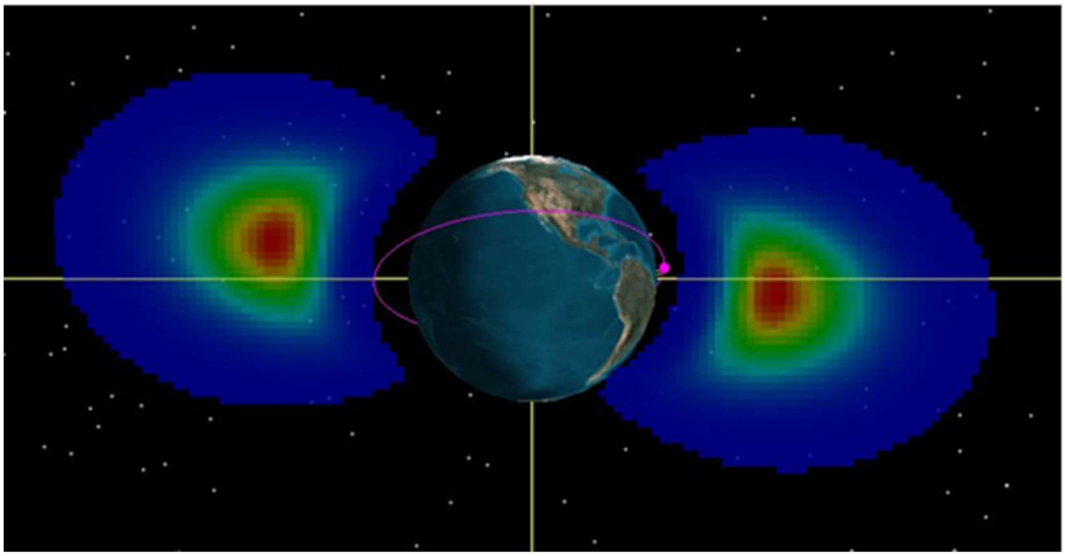

Figure 2. *Proton radiation flux cross-section for particles at 5.7 MeV based on the NASA AP8 model. Higher values are concentrated in the inner Van Allen radiation belt. (Figure courtesy of AER, Inc.)*

Radiation Models

IRENE (AE9, AP9, and SPM)

International Radiation Environment Near Earth (IRENE) is a radiation belt and space plasma specification model software suite that provides estimates of trapped energetic electrons, energetic protons, and space plasma from the AE9, AP9 and SPM component models, respectively. It is used in space system designs, mission planning, and other applications of climatological specification.

IRENE is based on 45 satellite-based data sets processed to create maps of particle fluxes along with estimates of uncertainties from imperfect measurements and space weather variability. These uncertainty estimates can be obtained as statistical confidence levels (e.g., the 50th and 95th percentile) for fluxes and derived quantities, supporting design trades.

The energy levels for the AP9 (proton) model range from 0.10 to 400 MeV. For the AE9 (electron) model, energy levels range from 0.04 to 10.00 MeV.

The IRENE model package (of AE9, AP9, and SPM) continues to be under active development in a collaboration led by the Air Force Research Laboratory (AFRL) which includes: Aerospace Corporation, Atmospheric and Environmental Research, Inc. (AER), Los Alamos National Laboratory (LANL), MIT Lincoln Laboratory (MIT-LL), and Boston College. More details about IRENE can be found at https://www.vdl.afrl.af.mil/programs/ae9ap9/ .

APEXRAD
APEXRAD is a radiation model based on data collected by the APEX Space Radiation Dosimeter to predict the amount of radiation received (dosage rate or total dose), providing dosing data from behind four shielding thicknesses (4.29, 82.5, 232.5, 457.5 mil Aluminum).

CRRESRAD
CRRESRAD is a radiation model based on data collected by the Combined Release and Radiation Effects Satellite (CRRES) Space Radiation Dosimeter to predict the amount of radiation received (dosage rate or total dose), providing dosing data from behind four shielding thicknesses (82.5, 232.5, 457.5, 886.5 mil Aluminum). The CRRESRAD database is divided into several activity levels: quiet refers to data obtained before the large 24-Mar-1991 storm, active refers to data obtained after the storm, and average refers to the average over the mission.

CRRESELE
CRRESELE is an electron-flux model that computes the energy differential omni-directional energetic electron flux at discrete energies using flux models constructed from data collected by the High Energy Electron Fluxmeter (HEEF) instrument flown on CRRES. It reports electron fluxes only for a specific set of energy levels (0.65, 0.95, 1.60, 2.00, 2.35, 2.75, 3.15, 3.75, 4.55, 5.75 MeV).

CRRESPRO
CRRESPRO is a proton-flux model that computes the energy differential omni-directional energetic proton flux at discrete energies, using flux models created from data collected by the proton telescope (PROTEL) flown on CRRES. It reports proton fluxes only for a specific set of energy values (1.5, 2.1, 2.5, 2.9, 3.6, 4.3, 5.7, 6.8, 8.5, 9.7, 10.7, 13.2, 16.9, 19.4, 26.3, 30.9, 36.3, 41.1, 47.0, 55.0, 65.7, 81.3 MeV). The CRRESPRO database is divided into two activity levels: quiet refers to data obtained before the large 24-Mar-1991 storm and active refers to data obtained after the storm.

AE8
AE8 is an electron-flux model that computes the energy differential omni-directional electron flux using the NASA AE-8 radiation belt models at user-specified energies between 0.04 and 7.0 MeV.

AP8
AP8 is a proton-flux model that computes the energy differential omni-directional proton flux using the NASA AP-8 radiation belt models at user-specified energies between 0.1 and 400 MeV.

ShieldDose2

ShieldDose2 is a radiation-transport model that uses the electron and proton fluxes computed by the flux models to estimate the absorbed total dose of a detector as a function of depth in a user-specified shielding material (Figure 3). For arbitrary proton and electron incident spectra, the ShieldDose2 model calculates the dose absorbed in small volumes of the detector materials covered by an aluminum shield of user-specified depth. Outputs include total and species dosage rates due to electrons, electron bremsstrahlung, and protons.

The spatial coverage of the various models can be generally described to depend upon two parameters derived from the magnetic field model: the McIlwain L-shell parameter (L, a measure that indicates a particle's drift shell in the magnetic field), and the ratio of the magnetic field strength B at the current position along a field line to

the minimum magnetic field strength at the equator Beq along the same line, expressed as B/Beq. The models' ranges of validity, expressed in L shell values, are given in Table 1.

Table 1. Ranges of validity of the various radiation environment models

	L	
Mode	Minimum	Maximum
IRENE (AE9/AP9)	0.98	12.4
IRENE (SPM)	2	10
APEXRAD	1.0	5.95
CRRESELE/PRO	1.0	8.0
NASA AE8/AP8	1.17	11.5

South Atlantic Anomaly (SAA) Transit

The South Atlantic Anomaly (SAA) is a region of space with an increased concentration of ionizing radiation due to the configuration of the Earth's magnetic field. Such radiation can damage spacecraft electronics and cause single event upsets (SEUs) that can impair the functioning of electronic components. Knowledge of when a satellite will be in the SAA is useful for mitigating the risk of damage to spacecraft electronics.

At low altitudes, the Earth's magnetic field is approximately a tilted dipole pattern. Energetic electrons and protons trapped in this field form the Van Allen Belts. Because the center of the magnetic dipole pattern is offset from the center of the Earth, a portion of the inner radiation belt is closer to the Earth in the South Atlantic region than elsewhere; therefore, this region is known as the South Atlantic Anomaly (SAA). At lower altitudes, SAA radiation is concentrated off the South Atlantic coast of Brazil and spans several hundred kilometers in altitude, with a latitudinal spread of

approximately 30° and a longitudinal spread of approximately 60°. With increasing altitude, the SAA region spreads eastward and westward until at approximately 1300 km altitude it completely encircles the Earth (Figure 3).

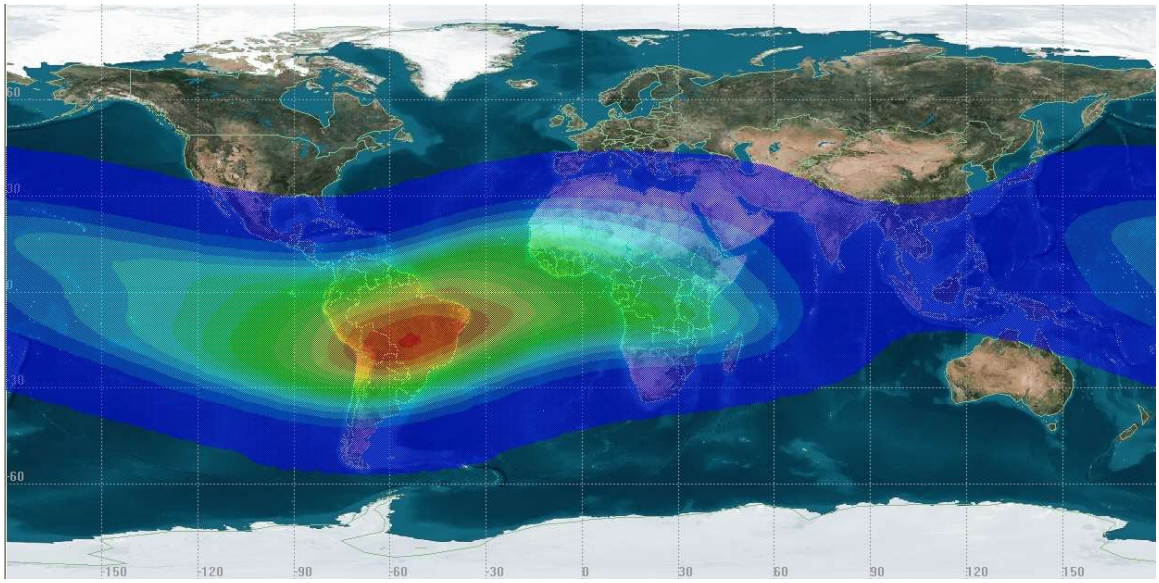

Figure 3. The South Atlantic Anomaly.
Flux intensity values at 1650 km altitude for protons > 23MeV.

The SAA model in SEET is based on data from the Compact Environment Anomaly Sensor (CEASE) proton-telescope detector flown on the Tri-Service Experiment (TSX-5) satellite during the epoch 2000 – 2006 (Ginet et al., 2007). The database, provided by the Air Force Research Laboratory (AFRL), consists of four sets of gridded integral energy flux values above each of four proton-energy flux thresholds: 23, 38, 66, and 94 MeV. The resolution of the data is 3 degrees for both latitude and longitude and 50 km in altitude, covering all latitudes and longitudes and ranging in altitude from 400 km through 1700 km.

SEET's South Atlantic Anomaly (SAA) Transit module computes the entrance and exit times of a given satellite through the SAA region, as well as the energy flux as a function of location. All flux-related output requires that the energy channel parameter (one of the four proton-energy thresholds) be specified; the user should select the appropriate energy channel (23, 38, 66, or 94 MeV) based on the nature and sensitivity of on-board instrumentation. Additionally, the model provides methods for retrieving SAA flux contours for specified energy channels and altitudes. The retrieved contour levels are mapped with respect to the maximum flux encountered for the particular energy channel and altitude; the contours that can be

requested are background flux level plus 3 standard deviations, tenth of maximum flux, or half of maximum flux.

Untrapped Radiation Environment

The near-Earth untrapped radiation environment consists of Galactic Cosmic Rays (GCR) and Solar Energetic Particles (SEP). GCRs originates from inter-stellar space but we are partially shielded by the Sun's magnetic field; their flux levels are relatively low, a few particles per cm2 per second, but are continuous. SEPs originate as occasional outputs from the Sun, through solar flares and coronal mass ejections (CMEs); these occur sporadically throughout the solar cycle, typically lasting several days, but sometimes at higher flux levels, on the order of tens of thousands of particles per cm2 per second. These highly energetic particles from GCR and SEP, consisting of both protons and heavy ions, can cause major disruptions to human technology (Feynman & Gabriel, 2000), such as single-event effects (SEE) in microelectronics. They also pose health risks to astronauts, as well as passengers and crew on airline flights over polar regions (Beck et al., 2005; Getley et al., 2005).

Galactic Cosmic Ray (GCR) Models

Galactic cosmic rays (GCR) are high energy charged particles originating from beyond the solar system (Bourdarie and Xapsos, 2008, Xapsos et al., 2013). They consist primarily of atomic nuclei that have been completely stripped of electrons. There is also a so-called "anomalous" cosmic ray component, or ACR, which is accelerated within the solar system at the shock where the solar wind meets interstellar space.

Number fluxes are dominated by protons and alpha particles, but all naturally occurring elements up through uranium are present. Fluxes tend to peak at around 1 GeV per nucleon. For energies below about 10 GeV per nucleon, fluxes are attenuated by the solar magnetic field and the solar wind.

SEET provides three different options for GCR models: Badhwar-O'Neill 2010 (BO10), CREME86, and ISO-15390. The primary differences between the models are the amount of data on which the model is based and the way they model the solar modulation. All three models calculate particle fluxes in free space outside the Earth's magnetosphere; no geomagnetic cutoff effects are currently applied. Therefore, SEET output for GCRs currently consists only of reports and graphs and no 2D or 3D graphics.

The three models are discussed briefly below.

Badhwar-O'Neill 2010 (BO10)

The Badhwar-O'Neill 2010 model (O'Neill, 2010) includes measurements of GCR flux from 1955 to 2010, spanning Solar Cycles 19 to 24. It is an improvement to the Badhwar-O'Neill 1996 model (Badhwar and O'Neill, 1996). The measurements are heavily based on data from the NASA Advanced Composition Explorer (ACE) Cosmic Ray Isotope Spectrometer (CRIS) that is currently measuring the low-energy (50-300 MeV/n) spectrum for all ions from lithium to nickel (see http://www.srl.caltech.edu/ACE/). It uses functions similar to those in ISO-15390 to determine the solar modulation.

CREME86

CREME86. The Cosmic Ray Effects on Microelectronics, or CREME86 model (Adams, 1987), was one of the first comprehensive models of GCRs. Energy spectra are based primarily on measurements of hydrogen and helium in the energy range 10 MeV/n to 100 GeV/n. For most other elements, fluxes are scaled from the helium spectrum using either a constant or energy-dependent factor. The solar cycle modulation is modeled as a sinusoidal variation with solar minimum in February 1975 and solar maximum in August 1980. Because the sinusoidal variation is not representative of the true solar cycle modulation, CREME86 should only be run for the solar extrema.

CREME86 can also include ACRs the model has options to assume whether the ACRs are singly- or fully-ionized.

Interplanetary Weather Index M

- M=1 (default): Provides best approximation to the galactic cosmic ray flux at the given date.
- M=2: The "anomalous" component, assumed fully ionized, is added to galactic cosmic rays.
- M=3: gives worst-case galactic cosmic ray fluxes that allow uncertainties in flux data and solar activity. These fluxes are so severe that they have only a 10% chance of being exceeded by actual fluxes at any moment.
- M=4: a singly-ionized "anomalous component is assumed. The singly-ionized particles are affected differently than fully-ionized particles by geomagnetic cutoff.

ISO-15390

The ISO-15390 model (ISO, 2004; Nymmik, 2000) has been adopted as an international standard for computing GCR spectra. GCR spectra are based on

measurements available up until about the year 2000. The model uses multi-parameter fits to relate the solar modulation to observed sunspot numbers. These fits account for the time lag between solar activity and the GCR flux at Earth; this time lag varies between about 8 and 15 months and depends on the phase and polarity of the solar magnetic field and on the magnetic rigidity of the particles.

Solar Energetic Particles (SEP)

Solar Energetic Particles (SEP) are protons and ions that originate in the solar wind. These particles pose a hazard to orbiting spacecraft (Feynman and Gabriel 2000, Dyer et al. 2004), particularly through internal charging of electronic components. During highly active years in the 11-year solar cycle, there is an increase in SEP flux driven by solar flares and shocks. Solar minimum years, meanwhile, produce low SEP levels.

Using the database of particle observations from the Interplanetary Monitoring Platform (IMP) satellites and Geostationary Operational Environmental Satellites (GOES), models have been developed to predict the cumulative particle fluence expected during the lifetime of a mission. Among these, the (Rosenqvist et al., 2005, 2007), an update to the JPL-91 model, and Emission of Solar Protons (ESP; e.g., Xapsos et al., 1998, 2000) models are implemented in SEET.

Descriptions of the models are as follows:

JPL-91 Model

In the JPL-91 model, (Feynman et al., 1990) characterized expected proton fluence for satellite design using observations obtained between 1963 and early 1991. Data were used from the IMP 1, 2, 3, 5, 6, 7, and 8 satellites, in addition to OGO 1. The estimate of total proton fluence during a mission is dominated by the probability of the occurrence of large events, associated with solar maximum years. The probability of a proton fluence being exceeded is characterized by a Poissonian distribution. The main parameter of importance is the average number of events occurring during the mission.

Rosenqvist et al. (2005, 2007) model

As an update to the JPL-91 model, the Rosenqvist et al. model includes data from the GOES satellites, with observations from January 1974 to May 2002. Updates were made to the mean and standard deviation of the probability distributions, as well as estimates of the average number of events expected during active years.

ESP Model

The ESP model uses a maximum entropy technique to determine the probability distribution for exceeding a fluence level during a mission (Figure 4). Also, the data source includes 3 complete solar cycles (20-22) of proton observations, with data from IMP 3, 4, 5, 7, and 8, as well as GOES 5, 6, and 7. Predictions are made for proton fluence from integral energy channels from >1 MeV through > 100 MeV. Additionally, this model includes a formulation of the worst-case event fluence expected.

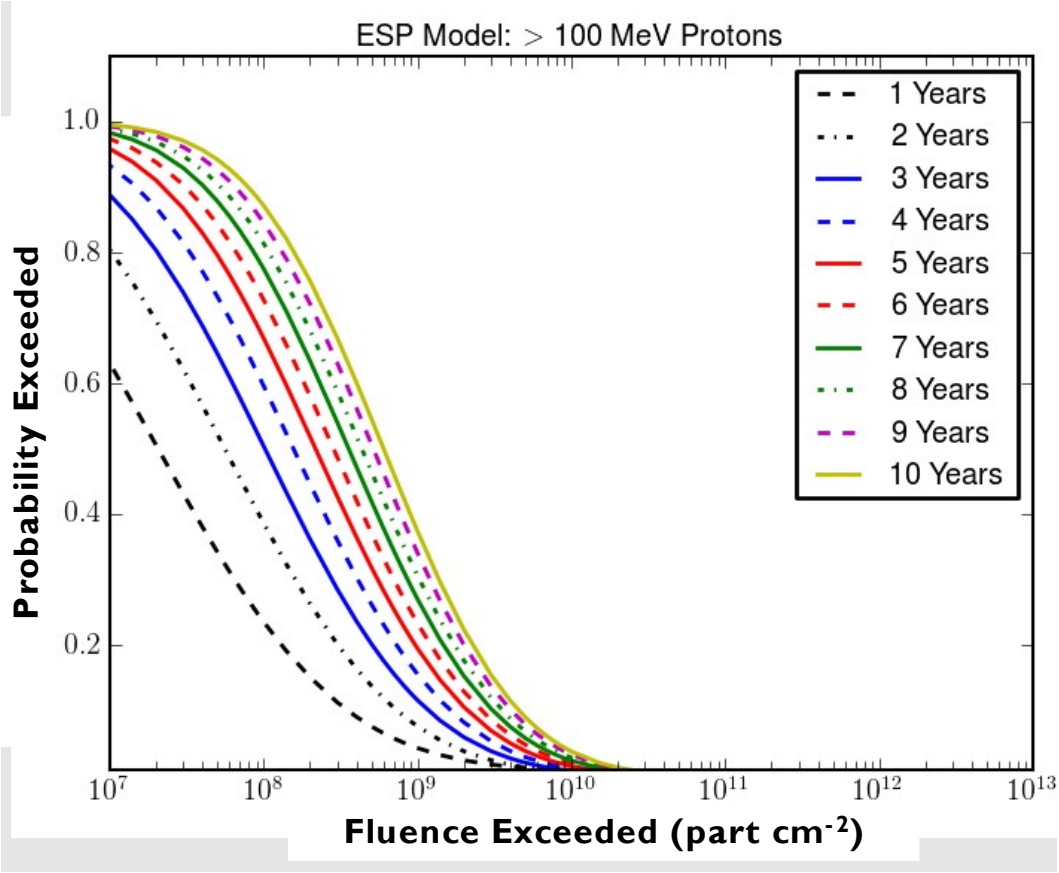

Figure 4. Probability of exceeding proton fluence level for a variety of mission lengths with the ESP model.

Particle Flux

SEET's Particle Flux module computes the probable number of small particles impacting a spacecraft along its orbit during a specified time period for particles originating from two environmental sources: naturally occurring meteoroids and man-

made orbital debris. The probable number of particles impacting can either be the total number or only those that would cause damage above a surface damage threshold level (pitting depth) specified by the user. Impact by these particles can cause significant damage to space vehicles when the total momentum (mass times relative velocity) of the impacting particles is large. The probable impact rate on a satellite is determined from the modeled particle environment (discussed below) and the cross-sectional area of the satellite (specified by the user). For impacts above the damage threshold, the type of surface material also plays a role and may be specified by the user. The probable total mass distribution of impacting particles may also be computed.[1]

Meteor Environment

Annual meteor showers occur when the Earth passes through the dust trails of the various cometary orbits. The timings of these showers are generally well established, though some irregular periods also occur. Most meteoroids consist of particles that have masses in the range 1 μg – 10 mg with a peak near 10 μg. Velocities can range between 12 km/s and 70 km/s. Two important characteristics of meteor showers are the radiant (the point in the sky where meteors from a specific shower seem to come from) and the Zenithal Hourly Rate (ZHR) – the number of shower meteors per hour an observer would see under a clear sky. Generally, the known showers are relatively weak, corresponding to a ZHR of 200 or less. However, occasionally a meteor storm occurs when the Earth passes through an unusually dense cometary dust trail. In those cases, the ZHR may be as high as 10,000 or more for a short time.

SEET's Meteor Environment model is largely based on a database of 50 parameterized annual meteor showers. This database is derived from a table of ten years of visual observations in both northern and southern hemispheres (Jenniskens, 1994). The Jenniskens database specifies each shower in reference to its date and level of its ZHR peak and radiant location. Algorithms are used to translate the database's visual meteor-shower observation rates to mass-dependent flux rates, producing a time-dependent anisotropic meteoroid flux model of 221 different particle types ranging in mass from 10^{-9} g and 10^{2} g. (McNeil, 1999; McNeil, 2001; Rendtel et al., 1995; Hughes, 1975). The modeled meteoroid flux environment is supplemented with an optional background flux due to sporadic meteors (interplanetary cosmic dust that is not associated with any particular meteor shower

[1] The probable total mass distribution of impacting particles should be used with caution since damage rates will depend on the momentum distribution of the impacting particles and the total mass collected is likely to be negligible.

or source direction) using a commonly used particle mass distribution profile (Love and Brownlee, 1993; Rendtel et al., 1995).

Debris Environment

Orbital debris consists of large cataloged trackable space objects (such as inactive satellites and spent rocket stages) and the numerous small objects originating from larger space objects (generated by accidental or deliberate explosions, collisions, fragmentations, and surface erosion). While large space objects are best modeled as points in space, the smaller objects are best modeled as a spatial distribution of particle size density in space and not as individuals. The spatial distribution and motion of the debris about the Earth is largely dependent on the orbital characteristics of the original parent body and the forces involved in its breakup.

SEET's Debris Environment model is based on the empirically-derived equations by Kessler (1989) that calculate the amount of the small orbital debris particle flux at a given time as a function of particle size, satellite average altitude, orbital inclination, and the average of the F10.7 solar activity index for the previous 13 months (the F10.7 index is an indicator of the amount of solar energy affecting the Earth's atmosphere extending back to 1947). This model includes portions that predict the general increase of space debris over time via a fixed annual net growth rate. An average impact velocity profile, as a function of orbital inclination, has been calculated from associated equations. These equations have been based on many years of general debris observations (both space- and Earth-based) and produce yearly-averaged debris-particle flux values.

Given the debris and/or meteoroid flux environment as defined by these models, the algorithms from McDonnell and Sullivan (1991) are used by the Debris Environment module to determine the amount of the particle flux that would be capable of causing damage to a user-specified satellite surface.

Vehicle Temperature

SEET's Vehicle Temperature module computes the mean equilibrium temperature of a spacecraft due to direct solar and reflected Earth radiation using simple thermal balancing equations (Tribble, 1995). SEET treats the spacecraft as a single isothermal node to determine the steady-state temperature, where the user specifies bulk thermal characteristics of the spacecraft. The temperature computations are based on models for either spherical objects, or planar objects with a specified orientation.

Spacecraft Energy Budget

Incoming radiation from the Sun or Earth can be either absorbed or reflected by opaque spacecraft material. Sources of emitted and absorbed energy, along with any internal heat-dissipation, must be accounted for when determining a spacecraft's thermal management system. Conservation of energy under thermal equilibrium requires that:

$$\text{Energy}_{\text{absorbed}} + \text{Energy}_{\text{dissipated}} = \text{Energy}_{\text{emitted}} \tag{1}$$

Here, positive energy dissipation refers to the radiation of internally produced heat energy resulting from the operation electrical or mechanical components. The total thermal radiation transferred into and out of a spacecraft will be a function of an object's surface reflectivity and emissivity, surface area, temperature, and geometric orientation with respect to other thermally participating objects. Absorptivity is the material property that represents the fraction of the incoming radiation that is absorbed (not reflected) by the material, independent of the incident angle of the radiation with the surface, while emissivity is the material property that represents the fraction of energy emitted relative to an ideal blackbody at the same temperature.

Using the conservation of energy from Eq. (1) with the Stefan-Boltzmann law, the average external temperature T0 of a spacecraft may be modeled as

$$\sigma_B T_0^4 = \left[\left(\frac{(Q_{Sun} + Q_{ER})\eta_0 + Q_i}{\varepsilon_0} \right) + Q_{IR} \right] \frac{1}{A_0} \tag{2}$$

where σ_B is the Stefan-Boltzmann constant, Q_{Sun} is the direct thermal power from the Sun, Q_{ER} is power due to sunlight reflected from the Earth, Q_{IR} is radiant infrared power emitted from the Earth due to its temperature, Q_i is power from heat produced by instrumentation inside the spacecraft, η_0 is the material absorptivity of the spacecraft, A_0 the total radiating surface area, and ε_0 is the surface emissivity of the spacecraft. All power sources contribute while the spacecraft is sunlit, but only the emissive-infrared component from the Earth QIR and internally-generated heat Q_i contribute while the spacecraft is in the shadow of the Earth.

Earth's Infrared Radiation

The Earth's atmosphere, cloud cover, and gas concentrations determine the absorbed portion of the incoming energy and emitted infrared energy. The albedo of the Earth is modeled the hemispherical average of the fraction of (visible or short wavelength)

solar energy reflected from the Earth back into space by the Earth's atmosphere, clouds, oceans, ice, and land surfaces.

Typically, 30% of solar energy at optical wavelengths may be reflected and thereby contribute to Q_{ER}. The remaining solar energy is absorbed by the atmosphere and Earth's surfaces, raising the Earth's temperature, and thereby contributing to QIR. The Earth's albedo, the power per unit area from the Sun ("solar constant"), and the spacecraft's distance from the Earth and Sun are therefore used in combination to estimate the radiated power affecting the temperature of the spacecraft. The expression for Q_{ER} affecting a sphere can be found in Cunningham (1961) and the expression for Q_{ER} affecting a plate can be found in Cunningham (1963). The expression for Q_{IR}, also a function of the distance from the Earth and Earth albedo, can be found in Stevenson and Crafton (1961) for both a sphere and a plate. Q_{Sun} is a function of solar flux, the model shape, and distance from the Sun (Griffin and French, 1991).

To determine the reflected incidence of incoming radiation, the user specifies a plate model or sphere model via the Shape Model parameter, depending on which shape best represents the spacecraft or spacecraft component to be analyzed. The cross-sectional area for a sphere or plate is also required, and a surface normal vector must be specified for the plate orientation, if applicable. The surface normal vector is defined as the orthogonal vector to the surface, pointing away from the planar surface.

Magnetic Field

The Earth's internal magnetic field (i.e., the geomagnetic main field) can be represented approximately as a magnetic dipole, with one pole near the geographic North Pole and the other near the geographic South Pole. The locations of the poles and the strength of the field vary over time, so standard coefficients that represent the geomagnetic field are adjusted periodically. These standard series of coefficients, together with their standard mathematical description, are known as the International Geomagnetic Reference Field (IGRF). The full description of the IGRF main field is a multi-pole spherical harmonic expansion containing over 100 coefficients:

$$V(r,\theta,\lambda,t) = R\sum_{n=1}^{N_{\max}}\left(\left(\frac{R}{r}\right)^{n+1}\sum_{m=0}^{n}\left(g_n^m(t)\cos(m\lambda)+h_n^m(t)\sin(m\lambda)\right)P_n^m(\theta)\right) \quad (2)$$

where r, θ, λ are geocentric coordinates, r is the distance from the centre of the Earth, θ is the co-latitude, (i.e. 90° minus latitude), and λ is the longitude, R is the IGRF reference radius (6371.2 km), $g_n^m(t)$ and $h_n^m(t)$ are the harmonic coefficients at time *t*, and $P_n^m(\theta)$ are the harmonic coefficients at time t, and are the Schmidt semi-normalized associated Legendre functions of degree n and order m.

The standard coefficients of the IGRF main field are maintained in tables having nodal values added about once every five years. Between these nodal epochs, the coefficients are linearly interpolated to approximate their slow change over time. For the five years after the most recent epoch, a linear secular-variation model of truncated degree is used for forward extrapolation (NGDC IGRF Web Site).

In addition to the main field, charged particles emitted from the Sun, called the solar wind, carry the interplanetary magnetic field outward from the Sun in all directions. The solar wind impinges on the Earth's main field, creating a magnetic draping effect that alters the basic dipole character of the near-Earth magnetic field at very high altitudes (Figure 5).

The contribution to the magnetic field due to the solar wind interaction is called the external field and is modeled separately. The optional external field model for SEET is the Olson-Pfitzer model (Olson and Pfitzer, 1977), which only depends on the local time of one's position of interest within the field (i.e., position relative to the direction of the Sun).

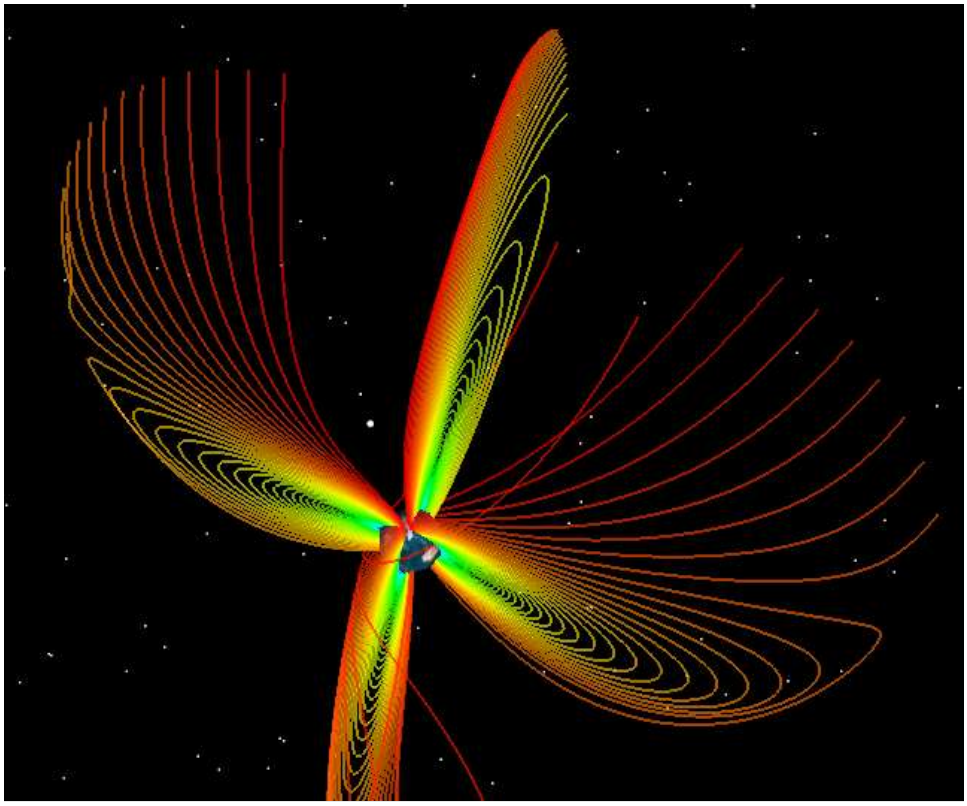

Figure 5. Sample Magnetic Field Lines showing draping (IGRF with Olson-Pfitzer external field).

The region in which the Earth's total magnetic field (main and external) exerts the dominant influence on charged particle motions is called the magnetosphere. Knowledge of the Earth's magnetic field is useful for satellite engineers and mission planners and operators because the magnetic field largely controls the distributions and motions of high energy charged particles within the magnetosphere: the Van Allen radiation belts, solar energetic particles, and galactic cosmic rays. Such high-energy particles penetrate spacecraft and often cause single event effects and long-term degradation of components due to radiation dosing effects (discussed in the Radiation Environment module section above). In low-Earth orbit, measurements of the local magnetic field on a spacecraft in conjunction with knowledge of the model field can also be used for attitude control. The magnetic field also plays a role in electromagnetic radiation propagation, directly for lower-frequencies (Hz-kHz), and indirectly for higher frequencies through its effects on charged particle distributions.

SEET's Magnetic Field module computes the full vector magnetic field and magnetic field lines using main-field and external-field model options selected by the user. The range of output is available from the Earth's surface out to a few tens of Earth radii (about 120,000 km). SEET can also compute the dipole L shell parameter - an

identification method for field lines based upon the dipole part of the magnetic field model, the McIlwain L shell parameter - an identification method for field lines (technically, particle drift shells) computed using adiabatic invariants, and B/Beq - the ratio of magnetic field strength at the current location to that at the magnetic equator along the same field line. Several Vector Geometry Tool modules are available for computing and visualizing the field, and tools are also available for computing field-line footprints on any altitude surface as well as determining magnetic conjugacy. Conjugacy is defined as two spatial locations being connected by the same field-line (to within a small user-specified threshold).

References

Adams, J. H., Jr, Cosmic Ray Effects on Microelectronics, Part IV, NRL Memo Rep. 5901, Naval Research Laboratory, Washington, DC, 1987.

AF-GEOSpace User's Manual Version 2.1 and 2.1P, AFRL/RVBS, 29 Randolph Rd, Hanscom AFB, MA 01731 (2006).

AFSPC Pamphlet 15-2, Space Environmental Impacts on DOD Operations, October 2003.

Badhwar, G. D., and P. M. O'Neill, "Galactic cosmic radiation model and its applications," Adv. Space Res., vol. 17, no. 2, pp. (2)7– (2)17, 1996.

Bell, J.T., and M.S. Gussenhoven, APEXRAD Documentation, PL-TR-97-2117 (1997), AD 331633.

Bourdarie, S., and M. Xapsos, "The Near-Earth Space Radiation Environment," IEEE Trans. Nucl. Sci., vol 55, No. 4, pp 1810 – 1832 (2008); doi: 10.1109/TNS.2008.2001409.

Brautigam, D.H., and J. Bell, CRRESELE Documentation, PL-TR-95-2128, Phillips Laboratory, Hanscom AFB, MA (1995), ADA 301770.

Cunningham, F.G. (1961), "Earth Reflected Solar Radiation Input to Spherical Satellites", NASA Technical Note, D-1099.

Cunningham, F.G. (1963), "Earth Reflected Solar Radiation Incident Upon an Arbitrarily Oriented Spinning Flat Plate", NASA Technical Note, D-1842.

FAA Website, Environmental Control and Life-support Subsystem (ECLSS), Section 4.4.1.3, Basic Principles of Thermal Control.

Feynman, J., G. Spitale, J. Wang, and S. Gabriel, Interplanetary Proton Fluence Model: JPL 1991, J. Geophysics. Res., 98, 13281 (1993).

Feynman J., A. Ruzmaikin, and V. Berdischevsky, The JPL proton fluence model: an update, JASTP, 64, 1679 (2002).

Fraser-Smith, A.C., "Centered and Eccentric Geomagnetic Dipoles and Their Poles, 1600-1985", Rev. of Geophysics, No. 1, pp. 1-16, (1987).

Ginet, G.P., D. Madden, B.K. Dichter and D.H. Brautigam, Energetic Proton Maps for the South Atlantic Anomaly, IEEE Radiation Effects Data Workshop, 23-27 July 2007.

Griffin, M.D., J.R. French (1991), Space Vehicle Design, American Institute of Aeronautics and Astronautics, Inc.

Grun, E., Zook, H.A., Fechtig, H.. Geise, R. H., 1985,"Collisional Balance of the Meteoritic Complex", Icarus, v.62, p. 244.

Heirtzler, J.R., "The Future of the South Atlantic anomaly and implications for radiation damage in space," Journal of Atmospheric and Solar-Terrestrial Physics, 64, p. 1701-1708 (2002).

Heynderickx, D., J. Lemaire, E. J. Daly and H. D. R. Evans, "Calculating Low-Altitude Trapped Particle Fluxes with the NASA Models AP-8 and AE-8", Radiation Measurements, Vol. 26, pp. 947-952 (1996).

Huston, S.L, G.A. Kuck, and K.A. Pfitzer, Low altitude trapped radiation model using TIROS/NOAA data, in Radiation Belts: Models and Standards, J.F. Lemaire, D. Heynderickx, and D.N. Baker (eds.), Geophysical Monograph 97, American Geophysical Union, 119, 1996.

ISO, "Space environment (natural and artificial) -- Galactic cosmic ray model," ISO 15390:2004.

Jenniskens, P., Meteor stream activity: I. The Annual Streams, Astronomy and Astrophysics, 287, 990-1013 (1994).

Kearns, K.J. and M.S. Gussenhoven (1992), CRRESRAD Documentation, PL-TR-92-2201, Phillips Laboratory, Hanscom AFB, MA, ADA 256673.

Kessler, D. J., Watts, A. J., Crowell, J. (1989), "Orbital Debris Environment for Spacecraft Designed to Operate in Low Earth Orbit", NASA TM-100-471.

Love, S. G., and D. E. Brownlee (1993), A Direct Measurement of the Terrestrial Mass Accretion Rate of Cosmic Dust, Science, 262, 550-553.

McDonnell, J.A.M., K. Sullivan (1992), "Hypervelocity Impacts on Space Detectors: Decoding the Projectile Parameters". In Hypervelocity Impacts in Space, ed. J.A.M. McDonnell (Canterbury: University of Kent), pp 39-47.

McNeil, W., "Problems in the Prediction of Meteor Shower Effects on the Atmosphere", 37th AIAA Aerospace Sciences Meeting and Exhibit, January 1999, Reno, NV.

McNeil, W.J., R.A. Dressler, E. Murad, "Impact of a Major Meteor Storm on Earth's Ionosphere: A Modeling Study", Journal of Geophysical Research, 106, 10,447-10,465 (2001).

Meffert, J.D., and M.S. Gussenhoven, CRRESPRO Documentation, PL-TR-94-2218, Phillips Laboratory, Hanscom AFB, MA (1994), ADA 284578.

NASA Preferred Reliability Practice guideline, "Earth Orbit Environmental Heating", No. GD-AP-2301, National Aeronautics and Space Administration, Goddard Space Flight Center, Greenbelt, MD.

NASA National Space Science Data Center (NSSDC) website URL: ftp://nssdcftp.gsfc.nasa.gov/.

NGDC Web Site, International Geomagnetic Reference Field URL: http://www.ngdc.noaa.gov/IAGA/vmod/igrf.html

Nymmik, R. A., "Time lag of galactic cosmic ray modulation: Conformity to general regularities and influence on particle energy spectra," Adv. Space Res., vol. 26, no. 11, pp. 1875–2000, 2000.

O'Neill, P. M., "Badhwar-O'Neill galactic cosmic ray model update based on Advanced Composition Explorer (ACE) energy spectra from 1997 to present," Adv. Space Res., vol. 37, pp. 1727–1733, 2006.

O'Neill, P. M., "Badhwar–O'Neill 2010 Galactic Cosmic Ray Flux Model – Revised," IEEE Trans. Nucl. Sci,, vol. 57, no. 6, pp 3148 – 3153 (2010); doi: 10.1109/TNS.2010.2083688.

Olson, W. P. and K. A. Pfitzer (1977), Magnetospheric magnetic field modeling, Annual Scientific Report, AFOSR Contract No. F44620-75-C-0033.

Rendtel, J., Arlt, R.,McBeath, A. (Eds.), 1995. Handbook for Visual Meteor Observers. The International Meteor Organization, Potsdam, Germany.

Seltzer, Stephen M. 1994, “Updated Calculations for Routine Space-Shielding Radiation Dose Estimates: SHIELDOSE-2,” National Institute of Standards and Technology Publication NISTIR 5477.

“Space Station Freedom Natural Environment Definition for Design” 1991, NASA SSP 30425 Rev. A, Chap. 8.

SPENVIS System Website, Background on Magnetic Field Models.

Stevenson, J.A. and J.C. Crafton (1961), “Radiation Heat Transfer Analysis for Space Vehicles”, ASD Technical Report 61-119.

Tribble, A.C. (1995), “The Space Environment: Implications for Spacecraft Design”, Princeton Univ. Press, Princeton, p. 24.

Tsyganenko, N.A., A Magnetospheric Magnetic Field Model with a Warped Tail Current Sheet, Planet. Space Sci., 37, 5-20 (1989).

Xapsos, M. A., C. Stauffer. T. Jordan, J. L. Barth, R. A. Mewaldt, "Model for Cumulative Solar Heavy Ion Energy and Linear Energy Transfer Spectra," IEEE Trans. Nucl. Sci., 54, pp 1085-1989, 2007.

Xapsos, M. A., G. P. Summers, J. L. Barth, and E. G Stassinopoulos, "Probability Model for Cumulative Solar Proton Fluences", IEEE Trans. Nucl. Sci., 47, pp 486-490, 2000.

Xapsos, M. A., P. M. O’Neill, and T. P. O’Brien, “Near-Earth Space Radiation Models,” IEEE Trans. Nucl. Sci,, vol. 60, no. 3, pp 1691 – 1705 (2013); doi: 10.1109/TNS.2012.2225846.